

Optimization of polarization rotators spectral response for broadband optical switching applications

Plinio Jesús PINZÓN, Isabel PÉREZ, Carmen VÁZQUEZ and José Manuel SÁNCHEZ-PENA

Grupo de Displays y Aplicaciones Fotónicas, Dpto. Tecnología Electrónica, Escuela Politécnica Superior, Universidad Carlos III de Madrid, C/ Butarque 15, 28911-Leganés, Madrid, Spain.

Contact name: P. J. PINZÓN (ppinzon@ing.uc3m.es).

ABSTRACT:

In this work, optimized designs of broadband polarization rotators based on cascaded nematic liquid crystal cells are presented. Visible spectral range (400 nm – 700 nm) is considered in the designs. A simple computational optimization approach, with performance comparable with more complex existing procedures, is used. Application of designed achromatic polarization rotators in the implementation of optical switches for wavelength division multiplexing in polymer optical fibers networks is also analyzed.

Key words: polarization rotator, liquid crystal devices, achromatic spectral response, computational optimization, optical switch.

1.- Introduction

Polymer optical fibers (POFs) application, in short distance communication networks, is increasing. To date, most used POF type is the step index POF (SI-POF), which presents an usable bandwidth limited to $14 \text{ MHz} \times 100 \text{ m}$ [1]. Initially, transmission with SI-POF has been realized with only one wavelength, however, in the last years, wavelength division multiplexing (WDM) has been proposed as one potential solution to expand the usable bandwidth of POF based systems [2], which requires the implementation of broadband optical devices (achromatic) for the VIS spectrum (400 nm – 700 nm).

Optical switches are key components in WDM networks. They selectively route optical signals delivered through one or more input ports to one or more output ports. Different technologies could be applied to route optical signals [3]. The final choice depends mainly on the optical network topology, switching speed and spectral range required.

Liquid crystal (LC) switches are based on polarization modulation in combination with polarization selective calcite crystals to steer the light [4], [5]. Main advantages of LC

technology include no need of moving parts for switch reconfiguration, low driving voltage and low power consumption. Its response time is in the order of several milliseconds, so it is ideal for protection and recovery applications and optical add/drop multiplexing, which demand fewer restrictions on switching time [3].

Usually, LC switches are based on twisted nematic LC cells (TNs), acting as polarization rotators (PRs), which are not achromatic. Therefore, their insertion loss and crosstalk are wavelength dependent. Achromatic TN based PRs require very thick cells, which dramatically increases the response time [6].

In this work, two achromatic LC based PRs are designed as part of 1×2 optical switches for POF-WDM networks. Proposed PR designs are done by using a simple computational optimization approach with a good performance versus more complex approaches. The designed LC switch allows redirecting the input beam to any of the two output ports, or splitting the input signal between the outputs ports [4] with adjustable split ratio, and without wavelength dependence in the VIS range.

2.- Polarization Rotators

PRs modify the orientation of a linear polarized beam in a specific angle, e.g. from being *x*-polarized (parallel to *x*-axis) to be *y*-polarized (parallel to *y*-axis), or a 90° rotation. Most common PR scheme consists of a single TN cell, see Fig. 1, while achromatic or broadband designs include TN cells, retardation plates and nematic homogenous LC cells (NHs), see Fig. 3.

2.1.- LC Devices Modeling

A LC cell operation is based on the optical birefringence, Δn , between the fast and slow axes of its molecules (slow axis is called *c*-axis). A NH cell, with thickness *d*, produces a phase delay between the polarization components of a light beam, with wavelength λ , that is given by:

$$\Gamma = 2\pi \frac{\Delta n d}{\lambda} \quad (1)$$

The LC *c*-axis angle respect to the cell surface is defined as tilt angle, θ , see Fig. 1c. Without applied voltage, *V*, NHs and TNs cells have $\theta = 0^\circ$. In a NH cell, the front and rear molecules have the same orientation angle, while in a TN cell there is a twist angle, ϕ , between them [7]. Therefore, NH cells are a particular case of TN cells with $\phi = 0^\circ$, and their Jones matrix representation [7] is given by:

$$W_H(\alpha) = R^{-1}(\alpha) \times \begin{pmatrix} e^{-i\frac{\Gamma}{2}} & 0 \\ 0 & e^{i\frac{\Gamma}{2}} \end{pmatrix} \times R(\alpha) \quad (2)$$

where $R(\alpha)$ is the rotation matrix of the LC *c*-axis orientation angle, α , respect to the *x*-axis, see Fig. 3; it is given by:

$$R(\alpha) = \begin{pmatrix} \cos(\alpha) & \sin(\alpha) \\ -\sin(\alpha) & \cos(\alpha) \end{pmatrix} \quad (3)$$

TN cells can be modeled as a stack of *N* NH layers, with constant *c*-axis orientation angles, varying a total twist angle ϕ , in increments of $\Delta\phi = \phi/N$. Then, the characteristic matrix of a TN cell [7], with its front *c*-axis oriented at an angle α and total twist ϕ , is given by:

$$W_T(\alpha) = R^{-1}(\alpha) \times \begin{pmatrix} \cos(\phi) & -\sin(\phi) \\ \sin(\phi) & \cos(\phi) \end{pmatrix} \times \begin{pmatrix} \cos(X) - i\frac{\Gamma \sin(X)}{2X} & \phi \frac{\sin(X)}{X} \\ -\phi \frac{\sin(X)}{X} & \cos(X) + i\frac{\Gamma \sin(X)}{2X} \end{pmatrix} \times R(\alpha) \quad (4)$$

where $X = [\phi^2 + (\Gamma/2)^2]^{1/2}$. The elements [1,1] and [2,1] of W_H and W_T represent the output *x*-polarized and *y*-polarized components, respectively, when the input is *x*-polarized.

2.2.- TN Based Polarization Rotator

A TN based PR consists of a TN cell bounded between linear polarizers, LPs, parallels to the LC front and rear *c*-axes. Most common design uses TN cells with 90° twist, e.g. input and output LP are parallel to the *x*-axis and *y*-axis, respectively (crossed LPs). In this configuration with $V = 0$ (Fig. 1.a.), from (4), an input *x*-polarized beam is transmitted with *y*-polarization direction, according to:

$$T_y = \left| \cos(B) - i\frac{\Gamma \sin(B)}{2B} \right|^2 \quad (5)$$

with $B = [(\pi/2)^2 + (\Gamma/2)^2]^{1/2}$. T_y from Eq. (5) is not an achromatic function, it presents periodic peaks at:

$$\frac{\Delta n d}{\lambda} = \frac{1}{2} \sqrt{4N^2 - 1} \quad \text{with } N = 1, 2, \dots \quad (6)$$

which are also called Mauguin minima [7]. Then, the transmitted beam polarization, at the TN cell output, is slightly elliptical. Ellipticity (*e*) is defined as the ratio of the *x*-polarization to the *y*-polarization component (a linear polarized beam has $e = 0$).

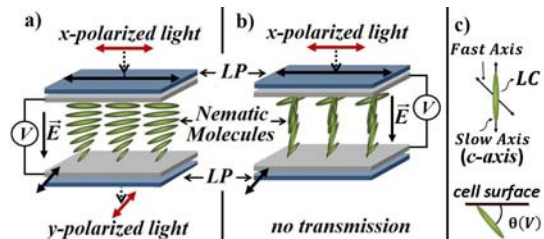


Fig. 1: TN cell based polarization rotator: a) $V < V_{th}$, b) $V \gg V_{th}$ and c) tilt angle definition.

On the other hand, when *V* is higher than a threshold value, V_{th} , the LC molecules are

tilted in the resulting electrical field direction (\vec{E}), $0^\circ < \theta < 90^\circ$, and they are parallel to \vec{E} when $V \gg V_{th}$, then $\theta \sim 90^\circ$, $\Gamma \sim 0$, there is not a polarization rotation and the light is blocked, as it is shown in Fig. 1.b.

Fig. 2 shows the transmittance or rotation efficiency, T_y , in the VIS range of two PRs, based on $5 \mu\text{m}$ and $10 \mu\text{m}$ width TN cells. The $5 \mu\text{m}$ TN cell based PR has $T_y \geq 90\%$. PR efficiency is improved to $T_y \geq 98\%$ using a $10 \mu\text{m}$ TN cell, which can be considered as an achromatic design if it is compared to that reported in [6], but the response time, τ , is increased by 300%, since $\tau \propto d^2$ [8]. Typically, a $5 \mu\text{m}$ TN cell has $\tau \sim 20 - 30 \text{ ms}$ [6].

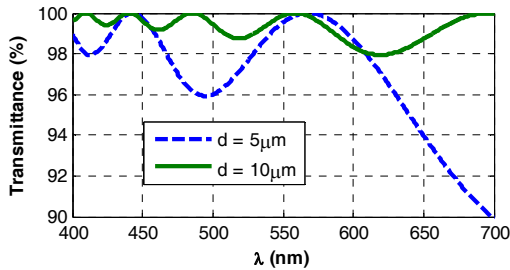


Fig. 2: Transmittance of a PR based on a TN cell with $d = 5 \mu\text{m}$ and $d = 10 \mu\text{m}$.

2.3.- State of the Art of Achromatic PRs

Many approaches have been proposed for designing achromatic PRs, with structures equivalent to that shown in Fig. 3. Some designs are based on multiple TN cells, as the one reported in [8] with experimental $T_y \geq 90\%$. And other designs are based on a single TN between NH cells [9], [10] or fixed retardation plates [6].

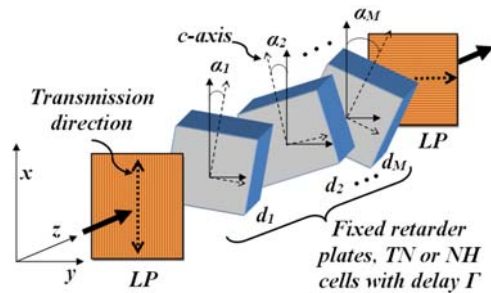


Fig. 3: Achromatic polarization rotator scheme, with M elements, where $d_1 \dots d_M$ are thickness and $\alpha_1 \dots \alpha_M$ are azimuth angles.

Those designs based on any optimization algorithm present the best performance. In [6] it is reported a PR scheme composed of a front retarder plate with $d_1 = 45.29 \mu\text{m}$ and $\alpha_1 = 89.96^\circ$, a TN cell with $d_T = 6.20 \mu\text{m}$, $\phi_T =$

90.12° and $\alpha_T = 0^\circ$ of E7 LC mixture, and a rear retarder plate with $d_2 = 4.83 \mu\text{m}$ and $\alpha_2 = -89.91^\circ$. The input LP is oriented at an angle $\beta = 1.64^\circ$. This PR presents $T_y \geq 97.8\%$ and it is designed after optimizing 7 variables ($\beta, \phi_T, \alpha_1, \alpha_2, d_T, d_1$ and d_2).

On the other hand, in [10] two design using E7 LC material are reported. Those results are shown in Fig. 4. The first design is based on three TN cells with crossed LPs, and the optimization includes thickness, azimuth and twist angles of each LC cell (9 variables). The optimal values are: $d_1 = 1.36 \mu\text{m}$, $\alpha_1 = -31.4^\circ$, $\phi_1 = 57^\circ$, $d_2 = 2.26 \mu\text{m}$, $\alpha_2 = -58.3^\circ$, $\phi_2 = 31.1^\circ$, $d_3 = 1.54 \mu\text{m}$, $\alpha_3 = 59.9^\circ$, $\phi_3 = 62.9^\circ$, for cells 1, 2 and 3, respectively. The device has $T_y \geq 99.95\%$, which represents the best rotation efficiency reported to date. In the second design, the cells 1 and 3 are NH (ϕ_1 and $\phi_3 = 0^\circ$) and the cell 2, that is placed between cells 1 and 3, is a TN cell. Then, 7 variables are used in the optimization, and the following optimal values are obtained: $d_1 = 2.49 \mu\text{m}$, $\alpha_1 = -79^\circ$, $d_2 = 3.94 \mu\text{m}$, $\alpha_2 = 10.9^\circ$, $\phi_2 = 66.5^\circ$, $d_3 = 2.47 \mu\text{m}$, $\alpha_3 = -11^\circ$. This second device has $T_y \geq 98.87\%$.

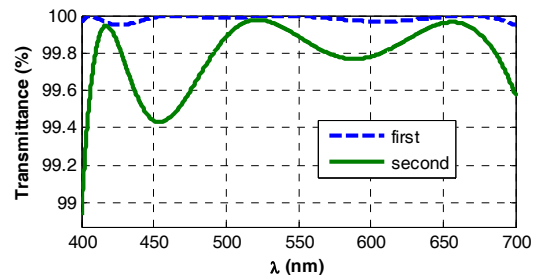


Fig. 4: Transmittance of the achromatic PRs reported in [10]: the first one uses three TN cells and the second one uses one TN cells and two NH cell.

Both designs used optimization algorithms and consider up to 9 variables. They also consider LC cells with very specific parameters, complicating the manufacture of the PR devices and increasing its tolerances. Optimization processes with fewer variables are often more effective and faster.

In the next section, very simple and effective PR achromatic designs are proposed. Their performance is as good as previous state of the art more complex designs. Commercial LC cells, which reduce manufacturing tolerances and facilitate the final device construc-

tion, are considered. The proposed optimization process allows also including the experimental characterization of LC devices [11], in order to obtain more precise results.

3.- Design of two Achromatic PRs

In this section, two achromatic PR designs based on the scheme of Fig. 3 are reported. Both designs use LC cells with E7 material, 5 μm thickness and 90° twists (for TN cells). An x -polarized input beam is considered and the losses are neglected.

The optimization process is performed by using a Genetic Algorithm (GA). The random nature of GA increments the possibility of finding a global minimum, moreover it allows implementing black-box function and the LC experimental characteristics, which can be discontinuous and non-differentiable, as part of the objective function. The proposed optimization problems consider only the c -axis orientation of each LC cell, $x = [\alpha_1, \alpha_2, \dots, \alpha_M]$ where M is the number of LC cells, see Fig. 3, and minimizes the next objective function:

$$F_{obj}(x) = \int_{400nm}^{700nm} |T_r - T_y(x)| d\lambda \quad (7)$$

where T_r is the required transmission level, $T_r = 1$.

3.1.- First Proposed Design

The first design is based on a TN cell, TN_1 , and a NH cell, NH_2 , with c -axis angles α_1 and α_2 , respectively. Then, the resulting transfer matrix is given by:

$$W_1 = W_H(\alpha_2)W_T(\alpha_1) \quad (8)$$

with transmittance, in the y -polarization direction, given by $T_{y_{opt1}} = W_1[2,1]$. The searching time was 5seg and the optimal values are $\alpha_1 = 16.5^\circ$ and $\alpha_2 = 17.1^\circ$, obtaining $T_{y_{opt1}} \geq 98.5\%$. This result, which uses only 2 LC cells, is better than the one reported in [6] ($T_y \geq 97.8\%$) and comparable to the one reported in [10] ($T_y \geq 98.87\%$). Both previous reported results are based on 3 elements (see section 2.3). On the other hand, α_1 and α_2 can be replaced by an average value, given by $\alpha_{av} = 16.8^\circ$, resulting in $T_{y_{opt12}} \geq 98.32\%$. This greatly simplifies construction of the device, and also allows joining both cells into a single

device. Fig. 5 shows the spectral response of $T_{y_{opt1}}$ and $T_{y_{opt12}}$.

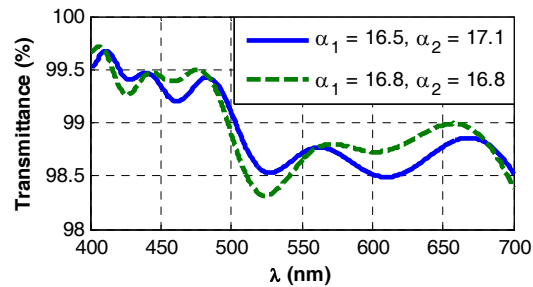


Fig. 5: Transmittance of the first proposed design: with optimal azimuth angles, $T_{y_{opt1}} \geq 98.5\%$ (solid line), and with the average azimuth angle, $T_{y_{opt12}} \geq 98.32\%$ (dashed line).

3.2.- Second Proposed Design

The second design is based on a TN cell, TN_2 , with c -axis angle α_2 , bounded by two NH cells, NH_1 and NH_3 , with c -axis angles α_1 and α_3 , respectively. Then, the resulting transfer matrix is given by:

$$W_2 = W_H(\alpha_3)W_T(\alpha_2)W_H(\alpha_1) \quad (9)$$

with transmittance in the y -polarization direction given by $T_{y_{opt2}} = W_2[2,1]$. The searching time was 10seg and the optimal values are $\alpha_1 = -13.8^\circ$, $\alpha_2 = 90.0^\circ$ and $\alpha_3 = -76.2^\circ$, obtaining $T_{y_{opt2}} \geq 99.74\%$, which is shown in Fig. 6. This result is better than the previous proposals based on similar configurations that optimize 7 variables [6], and it is comparable with that reported in [10] optimizing 9 variables (see section 2.3).

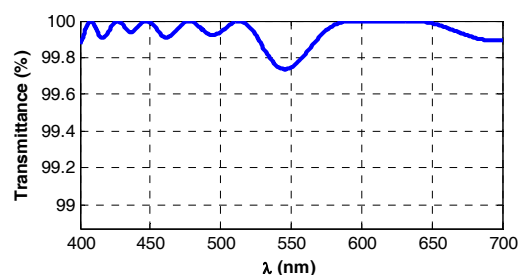


Fig. 6: Transmittance of the second proposed design, $T_{y_{opt2}} \geq 99.74\%$.

4.- Broadband optical switch design

The proposed PR designs allow a significantly improvement of the spectral response of LC optical switches, as in those previously reported [3], [4], [5], in a broadband range (400 nm–700 nm). This performance is required for implementing POF-WDM networks [2], and it can be achieved without

highly complicating their construction and using commercially available LC cells (fixed thicknesses).

A simple example of a 1×2 TN-LC optical switch is shown in Fig. 7. In this scheme, depending on the applied V , the input beam at Port S_0 is guided to Port S_1 or Port S_2 .

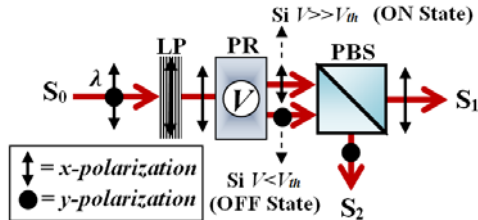


Fig. 7: Scheme of a 1×2 LC optical switch.

In order to show the improvement on the switch performance, the OFF state is analyzed (see Fig. 7). The performance on the ON state is mainly defined by LP and PBS characteristics. LP and PBS transmittances are not considered. In this scheme, the unpolarized input beam, with power P_0 , is x-polarized by LP, and on the OFF state, this polarization is rotated to be y-polarized by the PR, with efficiency T_y , and it is directed by PBS to S_2 . The output power at S_2 (active port), P_2 , is given by T_y and the output power at S_1 (inactive port), P_1 , is given by $T_x = 1 - T_y$.

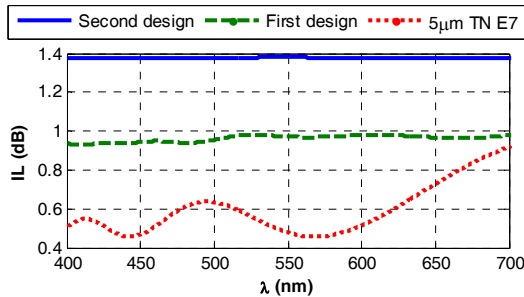


Fig. 8: Transmittance comparison of a TN base PR and the two proposed designs.

The ratio of P_2 respect to P_0 is defined as the insertion loss, $IL = -10\log_{10}(P_2/P_0)$. The implementation of PR devices with multiple LC cells increases the switch IL , but this is compensated by the switch IL uniformity, as it is shown in Fig. 8. In this figure, the IL of a TN based PR and the two PRs proposed designs are compared, considering 90% transmission in each cell.

Moreover, single TN based PRs allow output power level control [4] or variable attenuation, but for a specific wavelength, since its

transmittance is highly wavelength dependent for intermediate transmission levels, as it is shown in Fig. 9.

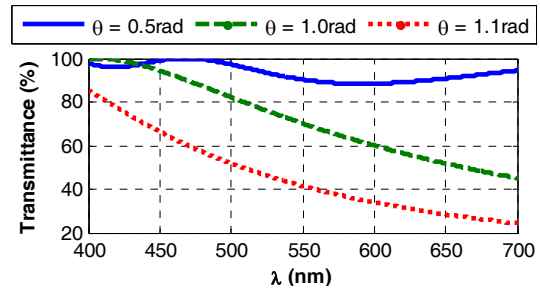


Fig. 9: 5µm TN cell based PR transmittance for three different tilt angles $\theta(V)$.

Proposed PR designs allow intermediate transmission levels, or variable split ratios, with good spectral uniformity in the VIS range, by applying different control voltages to each LC cell, as it is shown in Fig. 10. In this figure, 3 intermediate transmission levels of the second proposed design are shown. For simplicity, the control voltages are represented as the tilt angles θ_1 , θ_2 and θ_3 , for the cells NH_1 , TN_2 and NH_3 , respectively. Each tilt angle modifies the Γ of the respective LC cell [7] and their values are found with an optimization process similar to the one presented in section 2.4, with $x = [\theta_1, \theta_2, \theta_3]$ for $Tr = 0.9, 0.77$ and 0.66 .

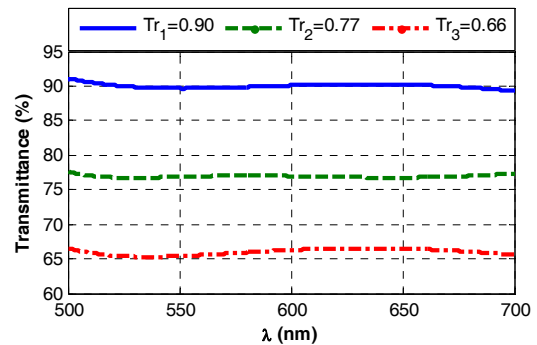


Fig. 10: Intermediate transmission levels of the second proposed design for $Tr_1 (x = [1.57 \ 0.93 \ 0.92]rad)$, $Tr_2 (x = [0.78 \ 1.13 \ 0.80]rad)$ and $Tr_3 (x = [1.17 \ 0.95 \ 1.16]rad)$. Variations are less than 1.84% (0.096 dB).

On the other hand, the ratio of P_1 (inactive port power) respect to P_0 is defined as cross-talk, $CT = 10\log_{10}(P_1/P_0)$. The CT of the Fig. 7 scheme, in the OFF state, is shown in Fig. 11, for a PR based in a TN cell of 5 µm and E7 mixture, and for a PR based in the second proposed design.

In WDM systems it is typically required that CT is less than -20 dB [3]. In Fig. 11, it is shown that the TN based PR presents $CT < -10$ dB in the VIS range and offers $CT < -20$ dB only for specific wavelengths (Mauguin minima) and for a specific bandwidth, e.g. in the 441 nm minimum the bandwidth with $CT < -20$ dB is limited to 30 nm, while in SI-POF networks the source bandwidths can be greater than 30 nm (LED sources). Therefore, the number of channels, their location and bandwidths are fixed. To allocate more channels it is required to have thicker cells, which increase dramatically the switching time.

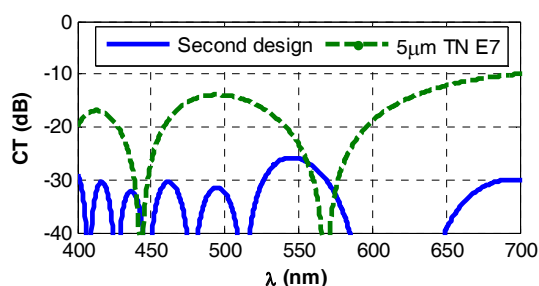


Fig. 11: CT of a LC switch, with PR devices based in a TN cell and in the second design.

As it is shown in Fig. 11, the second proposed design offers CT less than -25 dB in the range from 400 nm – 700 nm. Therefore, the number of channels, their wavelengths and bandwidths are not limited by the LC switch when achromatic PRs are implemented.

4.- Conclusion

Optimized designs of broadband PRs based on cascaded nematic LC cells are reported. A simple computational optimization approach is used. Without applying any voltage, the polarization rotation efficiency is greater than 0.9974. This behavior is comparable to more complex reported procedures and designs. Application of designed PRs in the implementation of optical switches for POF-WDM networks is also analyzed. The proposed design ensures CT values better than -25 dB and IL uniformity in the whole VIS range. It also allows intermediate transmission levels with good spectral uniformity (transmittance variations are $< 1.84\%$) in the VIS range.

Acknowledgements: This work has been sponsored by the Spanish CICYT (grant n°.

TEC2012-37983-C03-02) and CAM (grant. n°. S2009/ESP-1781).

References

- [1] R.T. CHEN and G.F. LIPSCOM, Eds., “WDM and Photonic Switching Devices for Networks Applications”, in Proceedings of SPIE3949, 2000.
- [2] M. JONCIC, M. HAUPT, U.H.P. FISCHER, “Standardization Proposal for Spectral Grid for VIS WDM Applications over SI-POF”, POF’2012, Atlanta, 2012.
- [3] Pedro CONTRERAS, “Advanced Devices Based on Fibers, Integrated Optics and Liquid Crystals for WDM Networks”, PhD Thesis, UC3M (2011).
- [4] P. J. PINZÓN, I. PÉREZ, C. VÁZQUEZ, J. M. S. PENA, “ 1×2 Optical Router With Control of Output Power Level Using Twisted Nematic Liquid Crystal Cells”, Mol Cryst. Liq. Cryst, 553, 36-43, 2012.
- [5] C. VAZQUEZ, J.M.S. PENA, S.E. VARGAS, L.A. ARANDA, I. PEREZ, “Optical router for optical fiber sensor networks based on a liquid crystal cell”, Sensors Journal, IEEE, 3, 513-518, 2003.
- [6] Qiong-Hua WANG, Thomas X. WU, Xinyu ZHU and Shin-Tson WU, “Achromatic polarization switch using a film-compensated twisted nematic liquid crystal cell”, Liquid Crystals, 31, 535-539, 2004.
- [7] Pochi YEH and Claire GU, “Optics of liquid crystal displays” (John Wiley & Sons, 2010)
- [8] Andrii B. GOLOVIN, Oleg P. PISHNYAK, Sergiy V. SHYANOVSKII, and Oleg D. LAVRETOVICH, “Achromatic Linear Polarization Switch for Visible and Near Infrared Radiation Based on Dual-Frequency Twisted Cell”, in Proceedings of SPIE6135, 2006.
- [9] Zhizhong ZHUANG, Young J. KIM and J. S. PATEL, “Achromatic linear polarization rotator using twisted nematic liquid crystals”, Appl. Phys. Lett. 76, 3995, 2000.
- [10] Qian WANG, Gerald FARRELL, Thomas FREIR and Jun SHE, “Optimal design of broadband linear polarization converters /switches”, J. Opt. A, 7, 47-50, 2005.
- [11] Baiheng MA, Baoli YAO, Tong YE, and Ming LEI, “Prediction of optical modulation properties of twisted-nematic liquid-crystal display by improved measurement of Jones matrix”, J. Appl. Phys. 107, 073107, 2010.
- [12] E7 LC mixture, <http://refractiveindex.info>.